FVIII regulates the molecular profile of endothelial cells: functional impact on the blood barrier and macrophage behavior

Marie Cadé, Javier Muñoz-Garcia, Antoine Babuty, Louis Paré, Denis Cochonneau, Karim Fekir, Mathias Chatelais, Marie-Françoise Heymann, Anna Lokajczyk, Catherine Boisson-Vidal, et al.

FVIII regulates the molecular profile of endothelial cells: functional impact on the blood barrier and macrophage behavior

Marie Cadé[1,2], Javier Muñoz-Garcia[2], Antoine Babuty[1,3], Louis Paré[4], Denis Cochonneau[2], Karim Fekir[5], Mathias Chatelais[5], Marie-Françoise Heymann[2], Anna Lokajczyk[6], Catherine Boisson-Vidal[6], Dominique Heymann[1,2,7,*]

[1] Université de Nantes, Saint-Herblain, France

[2] Institut de Cancérologie de l'Ouest, "Tumor Heterogeneity and Precision Medicine" laboratory, Saint-Herblain, France

[3] Department of Hemostasis, CHU de Nantes, France

[4] Université de Paris, CNRS, Institut Jacques Monod, UMR 7592, Paris, France

[5] ProfileHIT, Sainte-Pazanne, France

[6] Université de Paris, INSERM, Innovative Therapies in Haemostasis, F-75006, Paris, France

[7] University of Sheffield, Department of Oncology and Metabolism, Sheffield, UK

Running title: Impact of FVIII on endothelial cells

Total word count:

*** Corresponding author:**

Prof. D. Heymann
Institut de Cancérologie de l'Ouest
Blvd Jacques Monod
44805 Saint-Herblain cedex, France
Email: dominique.heymann@univ-nantes.fr

Abstract

Hemophilia A is an inherited X-linked recessive bleeding disorder caused by deficient activity of blood coagulation factor VIII (FVIII). In addition to a high risk of pathological bleeding, hemophilia patients show associated diseases including osteopenia, altered inflammation and vascular fragility. Nowadays, recombinant FVIII is proposed to treat hemophilia patients with no circulating FVIII inhibitor. Initially described as a coenzyme to factor IXa for initiating thrombin generation, there is emerging evidence that FVIII is involved in multiple biological systems, including bone, vascular and immune systems. The present study investigated: i) the functional activities of recombinant human FVIII (rFVIII) on endothelial cells, and ii) the impact of rFVIII activities on the functional interactions of human monocytes and endothelial cells. We then investigated whether rFVIII had a direct effect on the adhesion of monocytes to the endothelium under physiological flow conditions. We observed that direct biological activities for rFVIII in endothelial cells were characterized by: i) a decrease in endothelial cell adhesion to the underlying extracellular matrix; ii) regulation of the transcriptomic and protein profiles of endothelial cells; iii) an increase in the vascular tubes formed and vascular permeability *in vitro*; and iv) an increase in monocyte adhesion o activated endothelium and transendothelial migration. By regulating vascular permeability plus leukocyte adhesion and transendothelial migration, the present work highlights new biological functions for FVIII.

Key words: Factor VIII; endothelial cells; vascular permeability; angiogenesis; monocyte transendothelial migration; hemophilia

Introduction

Under physiological conditions, blood components interact permanently with the intact endothelium barrier in a dynamic manner. Leukocyte rolling, arrest and spreading on activated vascular endothelium under flow is controlled by a sequential process mediated by membrane-bound receptors for numerous factors including proteins, lipids, metabolites, cytokines, and hormones, and by specific junctional proteins and receptors that orchestrate cell-cell and cell-matrix interactions.[1] In addition, endothelial cells play a key role in the hemostatic cascade.[2] Vascular endothelium acts as a hemostatic barrier with potent anti-coagulant properties leading to the inhibition of platelet activation and aggregation. On the contrary, endothelial cells can respond to injury by switching from an anticoagulant to prothrombotic/procoagulant surface, initiating the coagulation cascade and thrombus formation.[3,4] Along with activating coagulation, endothelial cells play a part in recruiting leukocytes to the inflamed tissue, following already identified processes: tethering, rolling, arrest, adhesion strengthening, and transendothelial migration.[5]

Hemostasis is a dynamic process characterized by 3 consecutive steps: i) vasoconstriction to restrict blood loss and promote accumulation of procoagulants at the site of injury, ii) platelet activation and aggregation (platelet plug formation) through their contact with the subendothelial components and iii) coagulation cascade leading to thrombin activation and the formation of the fibrin clot.[4,6,7] The pivotal role played by FVIII in the coagulation cascade is now well-established.[6,7] The active form of FVIII (FVIIIa) acts as a cofactor in the tenase complex (FIXa/FVIIIa), making it possible to convert FX to its active form, FXa, through the serine protease FIXa.[9,10] FXa contributes to the prothrombinase complex with cofactor FVa, which catalyzes the conversion of prothrombin into thrombin. *In fine*, formed thrombin (FIIa) induces the conversion of fibrinogen into fibrin, resulting in clotting. The thrombin binds to protease-activated receptor (PAR)-1 and -4 expressed at the membrane of platelets and induces their activation and aggregation.[11] Even if thrombin is the main FVIII activator, FXa can also induce the activation of FVIII into FVIIIa. Activation by factor Xa cannot occur if FVIII is linked to von Willebrand Factor (VWF), which preserves FVIII integrity in the bloodstream and increases both its half-life and its bioavailability.[12] Although the cellular origin of FVIII remains uncertain and controversial, the liver plays a major role in its production. Other sites of production, including the lymph nodes, spleen, or lungs, have been identified.[13-15] Endothelial cells, like liver sinusoidal endothelial cells (LSECs), are the main cellular component capable of producing and secreting FVIII.[16-18] Endothelial cells also

express several receptors involved in the clearance of FVIII (e.g. the low-density lipoprotein receptor-related protein-1 or LRP1) and controlling its bioavailability.[4,19-22] Interestingly, in addition to its scavenger role, LRP1 is functionally related to the control of blood-brain barrier transcytosis, vascular permeability, and angiogenesis.[23-25]

Based on this observation, we hypothesized that FVIII may exhibit direct undetermined biological functions on endothelial cells. The aim of the present manuscript is to characterize the biological activities of FVIII on human endothelial cells. We then studied the impact of recombinant FVIII on the transcriptomic and protein profile of human umbilical vein endothelial cells (HUVECs), and on various biological functions of the endothelial barrier such as vascular permeability, vascular tube formation, the adherence/tethering/rolling of monocytes to the endothelium under physiological flow conditions, and their transendothelial migration.

Materials and Methods

Materials and methods

Reagents

The recombinant antihemophilic human FVIII (rFVIII, ADVATE®) and VWF (rVWF, VONVENDI®) used in all the experiments were kindly supplied by Takeda Pharmaceutical Company Limited (Bannockburn, IL, USA). Advate® was composed of the full-length human antihemophilic factor VIII (INN: octocog alfa) synthesized by a genetically engineered Chinese hamster ovary cell line. The recombinant human OPG (rOPG), TNF-α and IFN-γ were purchased from R&D Systems (Abingdon, UK) and MCP-1 and RANTES from Peprotech (Neuilly-sur-Seine, France).

Cell cultures

Human umbilical vein endothelial cells (HUVECs) were purchased from Lonza (CC-2519, Lonza), and cultured in endothelial cell growth medium-2 (EGM-2, Lonza). Cells were detached with Versene® (Millipore) and washed twice with PBS before use. Endothelial basal medium-2 (EBM-2, Lonza) was used for the "treated conditions" supplemented or not with 2% fetal calf serum (FCS), depending on the experiment. A single batch of FCS (Eurobio, CVFSVF 00-01, batch: 566809-0222/A) was used for all experiments. Endothelial colony-forming cells (ECFCs) were isolated from human umbilical cord blood, blood obtained from AP-HP, Hôpital Saint-Louis, Unité de Thérapie Cellulaire, CRB-Banque de Sang de Cordon, Paris, France (AC-2016-2759), expanded, and characterized as previously described.[26]

Cell adhesion assay

Cell adhesion was measured with the xCELLigence Real-Time Cell Analyzer (RTCA)-MP system (Acea Biosciences, Les Ulis, France). In a first set of experiments, HUVECs were seeded at 15,000 cells per well in an E-plate 96 (Roche Applied Science, Les Ulis, France) with EGM-2 medium in the presence or absence of increasing concentrations of rFVIII. In a second set of experiments, HUVECs were seeded in an E-plate 96 in EBM-2 supplemented with 5% of FCS, with or without increasing doses of rFVIII after overnight deprivation of growth factors in EBM-2 with 2% of FCS. Cell adhesion was monitored in real time for 2 h and the cell index was read automatically every 15 min. The impedance relative to the cells was reflected by the measurement of the Cell Index (CI) value, according to the following formula: CI = impedance at time point n-impedance in the absence of cells / nominal impedance value.[27]

RNA sequencing

After overnight deprivation of growth factors in EBM-2 with 2% of FCS, HUVECs were seeded in EBM-2 with 5% of FCS and treated or not with 10 IU/mL of rFVIII, 50 ng/mL of rWVF (50 ng/mL) or 100 ng/mL of rOPG for 7 hours. RNA extraction (all RIN > 9.0), library preparation and RNAseq analyses were performed with Active Motif (Carlsbad, California, USA). Briefly, 2 µg of total RNA was isolated using the Qiagen RNeasy Mini Kit and further processed in Illumina's TruSeq Stranded mRNA Library kit. Libraries were sequenced on Illumina NextSeq 500 as paired-end 42-nt reads. The reads were aligned with the hg38 reference genome STAR[28]and the count matrix was obtained using feature counts function from R package Rsubread[29]. The list of differentially expressed genes from DESeq2 output[30] was selected based on the adjusted p-value using the Benjamini-Hochberg procedure. Gene ontology, KEGG and Reactome pathway enrichment analyses were carried out using the open source Cytoscape software platform[31]. STRING database and MCODE Cytoscape's app were used to determine molecular complexes[32,33].

Protein profiling and flow cytometry

$5x10^3$ HUVEC cells per well in a 96-multiwell plate were cultured with EGM-2 supplemented with 2% of FCS for 96 h and treated with increasing doses of rFVIII (2.5, 5, 10 and 20 IU/mL) in the presence ("Inflammatory condition") or absence ("Non inflammatory condition") of 10 ng/mL of TNF-α or 20 ng/ml of IFN-γ for 48 h. The expression of a large

series of proteins (Supplementary Table 1) was studied after specific immunostaining using a FACSCanto™ II cell analyzer (BD Biosciences, Le Pont de Claix, France). A difference of 15% between the rFVIII treated and untreated cells was considered significant.

Cytoskeleton analysis using CytooChip™ micropatterns

Actin cytoskeleton, focal adhesion proteins (Phospho-Paxillin) and tight junctions (Zonula Occludens-1, ZO-1) were studied using Arena and Crossbow CytooChip™ (Grenoble, France) respectively. Both CytooChips™ were composed of micropatterns pre-coated with fibronectin (Sigma-Aldrich, Saint-Quentin Fallavier, France). HUVECs were seeded at 12,000 cells per well over Crossbow or Arena CytooChip™ in the presence or absence of increasing doses of rFVIII (0.62, 5, 10 IU/mL) for 18 h. Cells were then fixed for 10 min in PBS containing 1% formaldehyde, washed with PBS, and permeabilized with PBS containing 1% BSA (Sigma-Aldrich) and Triton 0.3 % (Sigma-Aldrich) for 20 min. Cells were then incubated with anti-vinculin Alexa Fluor 488 Phalloidin (1:1000 dilution) (ThermoFischer, Courtaboeuf, France), anti phospho-paxillin (#2541, 1:50 dilution) or anti ZO-1 antibody (#8193, dilution 1/100, Cell Signaling) overnight at 4°C. For the two last conditions, cells were rewashed and incubated for 1 h with goat anti-rabbit Alexa Fluor 555 antibody (1:2000 dilution; Thermofisher). Cells were washed in PBS containing 1% BSA, and mounted with ProLong antifade reagent (Molecular Probes, Eugene, OR, USA). Specimens were examined with immunofluorescence microscopy using a Nikon A1 RSi microscope (Nikon, Tokyo, Japan). Confocal images were analyzed with ImageJ software (NIH, USA).

Permeability assay

Permeability across HUVEC monolayers was measured using Transwell units (Boyden chambers) [8 µm pore size polycarbonate filter; Corning Costar; Pittston, PA, USA]. Transwell units were pre-coated with 40 µg/mL of human fibronectin and HUVECs were plated at the density of 70,000 per well (upper chamber). After 3 hours of incubation at 37°C, HUVEC monolayers were treated with increasing doses of rFVIII (2.5, 5, 10 and 20 IU/mL) or 10 ng/mL of TNF-α (positive control) for 1 h to 20 h and a solution of 250 µg/mL of 70 kDa FITC-labelled dextran was added simultaneously to the top chamber. Endothelial permeability was determined by measuring the flux of FITC-labeled dextran (through the HUVEC monolayer) in the medium collected from the bottom compartment using a Victor 3 reader (excitation 485 nm, emission 520 nm, Perkin Elmer, Villepinte, France).

Shear-flow adhesion assay

Mononuclear cells were isolated by density-gradient centrifugation from fresh peripheral blood mononuclear cells collected from healthy donors provided by the French blood bank institute (EFS) in accordance with an agreement with Paris Descartes University (C CPSL UNT n°12/EFS/064). Monocytes were isolated with the Monocyte Isolation Kit II (MACS Miltenyi Biotec, Paris, France) by negative selection. Flow adhesion experiments were conducted with a parallel-plate chamber in physiological shear stress conditions as previously described.[34-36] Three experimental conditions were tested: 1) control in the absence of rFVIII treatment; 2) monocytes treated with 10 IU/mL of rFVIII for 10 min; 3) HUVECs treated with 10 IU/mL of rFVIII for 24 h. Briefly, calcein-labeled freshly-isolated monocytes ($1x10^6$) were perfused on activated HUVEC monolayers for 15 min at 37°C at a shear rate of 50 s^{-1}. Adherent cells were visualized with phase-contrast microscopy. All experiments were observed in real-time and videotaped for offline analysis. Fluorescence micrographs of 28 random microscopic fields (obj. x10, 1 cm^2) were collected with Replay software (Microvision Instruments, France). The pattern of adhesion at 50 sec^{-1} was also analyzed to determine the number of tethering cells and adherent cells (immediate full arrest). Data were expressed as the number of adherent cells per field. In addition, adherent monocytes were tested for resistance to detachment from the modelled endothelium by increasing the flow rate from 50 to 5000 s^{-1} over 1 minute, and by counting the number of remaining adherent cells at one-minute intervals.

Monocyte-transendothelial migration assay

Assays were performed with Boyden chambers (Transwell, 8 µm pore size; ThinCert™, Greiner bio-one, Les Ulis, France). Membranes were coated with type I collagen (Sigma Aldrich) overnight at 4°C. HUVECs were grown in EGM-2 medium to confluency for 3 days until an endothelial monolayer was formed.[37] Monocytes were purified from anonymized whole blood samples (Centre de Ressources Biologiques - Tumorothèque of the Institut de Cancérologie de l'Ouest, DC-2018-3321, Saint-Herblain, France[38]) using a negative selection method (isolation Kit II, Miltenyi Biotec). After 3 days of HUVEC culture, purified monocytes were added to the upper part of the insert, in the presence or absence of 0.62 and 10 IU/mL of rFVIII in EBM-2 with 2% FCS. The lower chamber contained 15 ng/mL of MCP1 and 5 ng/mL of RANTES (Peprotech) as monocyte chemoattractants. Monocyte-transmigration was determined by the number of $CD14^+$ cells detected in the lower chamber with flow cytometry.

In vitro angiogenesis assays

Briefly, for the *in vitro* tube formation assay, ECFCs pretreated or not with 10 IU/mL of rFVIII for 6 h were seeded on Matrigel™ in EBM2. After 18 h of culture the cells were fixed with glutaraldehyde, stained with Giemsa and the total length of the tubules was measured under microscopy (original ×20).

Statistical analysis

Statistical analyses were performed using GraphPad Prism 6.0 software (GraphPad Software, La Jolla, CA, USA). Significance was determined using the Mann-Whitney, Kruskall-Wallis test, or One-way ANOVA. Error bars show mean ± standard error of the mean. A *p*-value ≤ 0.05 was considered statistically significant.

Results

FVIII lowers endothelial cell adhesion

The effects of rFVIII on HUVEC adhesion to the underlying extracellular matrix were studied by measuring the cellular impedance dynamically followed by the xCELLigence RTCA system. As shown in Figure 1, rFVIII significantly decreased HUVEC cell adhesion to the electronic E-plate surface compared to the untreated cells. In EGM2 medium, while 1, 2 and 5 IU/mL of rFVIII did not modulate HUVEC adhesion, 10 IU/mL reduced the cell index by 1.01 (± 0.11) after 2 h of treatment compared to the control (Figure 1A). When cultured in the growth factor deprived of EBM2 medium, rFVIII significantly decreased the cell index ($p<0.05$, Figure 1B). A decrease of 0.28 (± 0.03) and 0.33 (± 0.013) in the cell index was observed after treatment with 1 IU/mL and 10 IU/mL of rFVIII for 2 h respectively. The maximum effect of rFVIII on cell adhesion was observed at 10 UI/mL (data not shown).

FVIII, but not OPG and VWF, modulates the transcriptomic profile of HUVECs

To better characterize the functional impact of FVIII on endothelial cells, we analyzed the differential transcriptomic profile of HUVECs treated with recombinant factor using a comparative RAN-sequencing (RNA-seq) approach (Figure 2). Principal component analysis (PCA) demonstrated that rFVIII-treated HUVECs showed a differential transcriptomic profile compared to both VWF- and OPG-treated HUVECs, and to the untreated control cells, with inter-experiment variability reflecting the variability between HUVEC batches (Figure 2A). rFVIII induced a reproducible effect in all HUVEC batches assessed. Hierarchical clustering

confirmed this observation and identified 563 genes (|log2FC| > 1, p value adjusted <0.05) that were significantly differentially expressed in the presence of rFVIII (Figure 2B-D). A total of 168 and 395 genes were under- and overexpressed respectively. Thirty-one genes were modulated by a fold-change of more than 2 (|log2FC| > 1, p value adjusted <0.05) (Figure 2D**)**. Functional analysis of these genes was carried out using Cyoscape software and the SRING database (Figure 2E) and the most differentially expressed genes were related to functional pathways involved in tube morphogenesis, cell adhesion/migration, and immune response (Figure 2D, Supplementary Figure 1).

FVIII regulates the protein expression related to cell adhesion

A protein profile analysis of HUVECs was performed with flow cytometry under physiological or inflammatory conditions (Supplementary Figure 2). HUVECs were then treated with or without increasing doses of rFVIII (2.5, 5, 10 and 20 IU/mL) ("basal condition") or inflammatory cytokines 10 ng/mL of TNF-α and 20 ng/mL of IFN-γ to mimick the "inflammatory condition".[39,40] In the basal condition, rFVIII modulated the expression of cell adhesion molecules (ICAM-1, VCAM-1 and E-Selectin) at the HUVEC surface, confirming the data obtained by RNAseq (Table 1). E-Selectin was modulated from 2.5 IU/mL (+18.2%). E-Selectin and VCAM-1 expressions were simultaneously increased at 5 IU/mL of rFVIII (+ 26.9% and 20.6 % respectively) whereas ICAM-1 and VCAM-1 were upmodulated at 10 IU/mL of rFVIII (+16% and 20.3% respectively). At 20 IU/mL of rFVIII, ICAM-1 was increased by 32% compared to the untreated cells. The complementary functional pathways regulated by rFVIII in HUVECs were:

- the immune response (increase in TNFR1, TLR4 and MICA/B in the basal condition; in the inflammatory condition: increase of HLA-1 correlating with the increasing doses of rFVIII, decrease in HLA-2; upmodulation of CD137L and HVEM by 33.4% and 17.4% respectively with 5 IU/mL of rFVIII in the inflammatory condition),
- reorganization of the cytoskeleton and cell adhesion/migration (decreased expression of tight junction proteins such as ZO-1 and Claudin-1 in the presence of 5 IU/ml of rFVIII by 15.7% and 20.8% respectively; upmodulation of CD29 expression by 38.3% in the presence of 20 IU/ml),
- coagulation/vascular permeability: increase in CD41 and EPCR in the basal condition,
- regulation of lipid metabolism: increase in LDL metabolism associated with an increase in LDL uptake and LDL degradation by 37.9% and 26.9% respectively in the presence of 20 UI/mL of rFVIII.

Organization of the actin cytoskeleton and PAX phosphorylation are regulated by FVIII in endothelial cells

We first analyzed the functional impact of rFVIII on vascular tubule formation *in vitro* (Supplementary Figure 3). ECFCs were incubated overnight in starvation medium (EBM2 + 2.5% FCS) and stimulated for 6 h with 10 IU/mL of rFVIII in basal medium (EBM2 + 5% FCS) before seeding on Matrigel® for 18 h. The tubular network was significantly more extensive in the presence of rFVIII compared to the control cells (54 418 ± 1939 μm in the presence of rFVIII vs 40 418 ± 5509 μm for the control, $p<0.001$).

Actin fibers (F-actin) form a dynamic network associated with the inside cell membrane, which defines cellular shape and plasticity, controlling in particular key cellular process such as migration, endocytosis, division, and phagocytosis.[41,42] This cytoskeleton is connected to the extracellular matrix by focal adhesions, protein complexes that enable signaling, and cell adhesion.[43] In a second step we then studied organization of the cytoskeleton of HUVEC cells using crossbow CytooChip™. After 18 h of treatment with or without rFVIII, actin fibers were detected with immunocytochemistry (Figure 3). In the retraction zone of endothelial cells, the total stained surface of the stress fibers was significantly decreased in the presence of rFVIII (Figure 3 A,B). The total stained surface of stress fibers was 721.6 ± 32.6 μm² in the presence of 10 IU/mL of rFVIII compared to 930.8 ± 55.7μm² in the control group ($p < 0.01$). Similarly, the fiber-stained surfaces were significantly decreased after treatment in the retraction zone (Figure 3B). In the protrusion zone, the total stained surfaces of the actin network were also significantly decreased in the presence of rFVIII (Figure 3B). At 0.62 IU/mL, rFVIII significantly reduced the surface of the actin network (885.4 ± 97 μm² after treatment compared to 1335.8 ± 101 μm² without any treatment, $p < 0.001$) and 10 IU/mL of rFVIII decreased the corresponding surface by approximately 18% (1119.8 ± 50.9 μm², $p < 0.05$). Measuring the stained surfaces of each fiber confirmed this observation.

We then analyzed the phosphorylation levels of PAX in HUVECs polarized on fibronectin-precoated micropatterns (Figure 3C). As shown in Figure 3D, a significant decrease in the total stained surface of P-PAX was observed in the retraction zone after treatment with rFVIII (66.2 ± 3.6 μm² in the presence of 10 IU/mL of rFVIII compared to 89.7 ± 4.8 μm² in the control cells, $p < 0.001$). Similarly, the number of phosphorylated events was significantly lower in rFVIII-treated cells (25.4 ± 1.4 in the presence of 0.62 IU/mL of rFVIII compared to 32 ± 1.6 control cells) with no modification to the perimeter of each event. In the protrusion zone, in contrast to the retraction zone, the number of phosphorylated events was significantly

upmodulated by 0.62 IU/mL of rFVIII (35.3 ± 1.9 P-PAX events without treatment compared to 85.2 ± 5 in the presence of rFVIII, $p < 0.001$) (Figure 3E). This increase was associated with a significant decrease in the mean staining surface of the phosphorylated events (12 ± 1.7 μm^2 without treatment and 4.5 ± 0.5 μm^2 in the presence of rFVIII).

Functional impact of FVIII on vascular permeability, monocyte adhesion, and transendothelial migration

RNAseq and protein profiling identified molecules (e.g. ICAM1, VCAM1 and E-selectin) significantly regulated by rFVIII that may be involved in vascular permeability, adhesion, rolling, tethering and the transmigration of leukocytes.[44-46] The functional impact of rFVIII was thus assessed in the various physiological parameters.

FVIII increases vascular permeability

Vascular permeability was measured by the diffusion of FITC-labeled dextran through preformed HUVEC endothelium, treated or not with increasing doses of rFVIII or TNF-α as a positive control. As shown in Figure 4A, rFVIII increased vascular permeability in a dose-dependent manner. Whereas 2.5 and 5 IU/mL of rFVIII did not modulate the FITC-labeled dextran flux, 10 and 20 IU/mL of rFVIII increased vascular permeability by 75% compared to the untreated control and was similar to the positive control (Figure 4A, $p < 0.05$). Zonula occludens-1 (ZO-1) protein belongs to the protein families involved in the maintenance of the endothelial barrier.[47,48] We studied the effect of rFVIII on the expression of ZO-1 in HUVECs using arena CYTOOChip® (Figure 4B). The total ZO-1 stained surface was 1049.14 ± 43.29 μm^2 in untreated cells compared to 394.16 ± 20.35 μm^2 in the presence of 5 IU/mL of rFVIII ($p < 0.0001$) (Figure 4B). Similarly, at the same concentration, the staining surface per event ($p < 0.05$) and the number of events observed ($p < 0.01$) were significantly reduced. Overall, these data demonstrate that rFVIII significantly downmodulated ZO-1 expression in HUVECs.

rFVIII promotes monocyte rolling and adhesion to activated HUVEC monolayers under physiological shear stress conditions

We next investigated whether rFVIII had a functional impact on monocyte adhesion to the endothelium, under physiological flow conditions. Freshly-isolated human monocytes were stimulated for 10 min with 10 IU/mL of rFVIII in medium supplemented with 5% FCS, prior to adhesion. A monocyte adhesion assay was also performed on endothelium monolayers

pretreated with 10 IU/mL of rFVIII for 24 h. We used a flow-based adhesion assay using HUVEC monolayers to investigate the binding of monocytes to an activated preformed endothelium. The experimental conditions used mimicked the shear forces encountered by leukocytes adhering to vascular endothelial cells *in vivo*. As shown in Figure 5A, pre-treatment of endothelial cells with rFVIII significantly increased the number of rolling monocytes at a shear rate of 50 sec^{-1} (15.3 ± 0.24 in the presence of 10 IU/mL of rFVIII versus 6.8 ± 0.2 monocytes/sec for the untreated cells, $p<0.001$). Similar results were obtained when monocytes were pretreated with rFVIII (14.2 ± 0.22 monocytes/sec, $p < 0.001$) (Figure 5A). In contrast, the effect of rFVIII on monocyte tethering was comparable in all the experimental conditions tested (Figure 5A). Monocyte resistance to detachment was similar at higher shear stress (up to 2500 s^{-1}) in all conditions assessed (Supplementary Figure 4). The number of adherent monocytes was counted at the end of the perfusion process and confirmed the effect of rFVIII on monocyte rolling observed above (Figure 5B). The number of pretreated monocytes adhering to rFVIII increased 1.8-fold compared to the control (279.2 ± 17.9 monocytes per field versus 151.5 ± 10.5, $p> 0.0001$). Similarly, the number of adherent monocytes markedly increased when monocytes were pretreated with 10 IU/mL of rFVIII (535.9 ± 26.8 adherent monocytes per field, $p < 0.0001$) (Figure 5B). Interestingly, monocyte adherence to endothelium monolayers was significantly speeded up when monocytes were pretreated with rFVIII (Supplementary Figure 5).

Monocyte migration through HUVEC endothelium is modulated by rFVIII

Based on the functional regulation of monocyte adhesion to HUVEC endothelium by rFVIII, we then studied the transendothelial migration of human monocytes isolated from 6 donors and cultured in the presence of 0.62 and 10 IIU/mL of rFVIII for 4.5 h or 20 h (Figure5C). The results revealed the heterogeneous response of isolated monocytes to rFVIII. rFVIII stimulated monocyte transendothelial migration in 4 donors (donors 1, 2, 4 and 6) with differential sensitivity. rFVIII increased transendothelial migration from 0.62 IU/mL of rFVIII for donors 1 and 6 and from 10 IU/mL for donors 2, and 4.

Discussion

FVIII is a blood-clotting protein that plays a prominent role in the coagulation cascade as a cofactor for FIXa. In addition to being the main source of FVIII currently identified, endothelial cells express a series of scavenger receptors that control the bioavailability of this factor and that are suspected of being associated with specific vascular functions, such as permeability and angiogenesis.[19,23-25] The potential activities of FVIII in endothelial cells

remain poorly characterized. The present work studied the effects of recombinant FVIII (rFVIII) on HUVECs and demonstrated its impact on transcriptomic regulation and the protein profile of endothelial cells. Correlating with the gene and protein expression profiles modulated by rFVIII, rFVIII regulated the polarization of endothelial cells. rFVIII also upmodulated vascular permeability *in vitro*, the adhesion of monocytes to a pre-formed endothelium, and transendothelial migration of human monocytes. Overall, these results give new insights into both the implication of rFVIII in the biology of endothelial cells and its functional impact in hemophilia patients.

An xCelligence real-time adhesion assay demonstrated that rFVIII downregulated the adhesion potential of HUVECs. Complementary investigations based on microscopic observation of HUVEC cultures on CytooChip™ micropatterns, which allow normalization of cell polarity and internal cell organization, revealed the role played by FVIII in regulating stress actin fibers and PAX phosphorylation. Cellular adhesion results from the cooperation of several molecular protagonists (e.g. integrins and cell adhesion molecules) linking the cytoskeleton and the extracellular matrix (ECM) and then leading to the formation of dynamic adhesion structures.[49,50] The binding of integrins to the ECM results in the formation of focal adhesions (FA) associated with the phosphorylation of paxillin (PAX), a focal adhesion-associated phosphotyrosine-adaptor protein, and the assembly of actin fibers necessary for stabilizing and strengthening the interaction between cells and the ECM.[51-55] FA mature with the following dynamic steps: i) the formation of small (< 1 μm in diameter, lifetime: 60 seconds) so-called nascent adhesions; ii) nascent adhesions mature into focal complexes which are larger (1-2 μm in diameter) and less dynamic (lifetime: a few minutes); iii) FAs from the final maturation of focal complexes and characterized by large structures that are 2 μm wide and 3 to 10 μm long, with a long lifetime (30 to 90 minutes) and connected to actomyosin stress fibers.[50,51] rFVIII decreased the total phospho-PAX stained surface and the number of phosphorylated events in the retraction zone, which may reflect lower PAX activity and disturbed disassembly of the FAs.[46-48] In the protrusion zone, rFVIII induced the opposite effect and increased the number of P-PAX events. These results may reflect an increase in incipient adhesion formation at the level of the protrusion zone, where lamellipods form, and may favor cell migration. Nascent adhesions form in front of migrating cells.[51] These data may appear contradictory with regard to cell migration, but the discrepancy may be explained by the sequential phases in the cell migratory cycle. A migratory cycle is divided into 4 stages: protrusion, adhesion, contraction, and retraction.[51] The protrusion step corresponds to the formation of a thin lamellipod by the actin network. The adhesion stage

coincides with the adhesion of the lamellipod to the ECM, forming incipient adhesions at the front of these structures, and FAs at the cell rear. The actin stress fibers organize themselves from these FAs and connect themselves to the nascent adhesions. Maturation and growth of the focal complexes in FAs are dependent on actin tensile forces and extracellular stresses. The actin stress fiber contraction step then strengthens the FAs in the front of the cell, and weakens those at the rear. This contraction induces the forward movement of the cell body. Finally, the retraction step corresponds to the detachment of the FAs from the rear of the cell, allowing the retraction of the rear membrane.[51,52-55] In the presence of rFVIII, HUVECs may be blocked at the intermediate stage between protrusion, possibly explaining the formation of incipient adhesions at the front, associated with stronger adhesion at the rear. In addition, rFVIII induced a rearrangement of the actin network, characterized by lower density and smaller fibers both in the protrusion zone and the retraction zone. This information concurs with an increased formation of nascent adhesions in the presence of a low dose of rFVIII where the actin network initiates its early stages of formation. Overall, our data demonstrated the modulation of HUVEC adhesion and migration properties by rFVIII.

Actin stress fibers are also anchored to adherence junctions which control cell-cell adhesion, endothelial permeability, and metabolite/nutrient/cellular exchanges through the endothelial barrier.[42,62,63] rFVIII increased endothelium permeability, monocyte adhesion, and transmigration. ZO-1 belongs to the zonula occluding family, which are tight junction-associated proteins that establish a link between the occluding transmembrane protein and the actin cytoskeleton.[64] The tight junctions limit molecular and cellular transfers through the paracellular space and play a part in cell polarization and endothelial barrier formation.[47,65] The downmodulation of ZO-1 expression coincides with the increase in vascular permeability induced by rFVIII. In addition to modulating ZO-1 expression, rFVIII upmodulated several key adhesion molecules, including ICAM1, VCAM1 and E-selectin, suggesting an activation mechanism for HUVEC cells induced by FVIIIr. ICAM1, VCAM1 and E-selectin are involved in the process of leukocyte transendothelial migration that integrates: i) the tethering and rolling of leukocytes over the endothelium, ii) leukocyte activation, iii) leukocyte arrest and iv) leukocyte migration across the endothelium.[66,67] E-selectin is involved more particularly in step 1, while ICAM1 and VCAM1 are preferentially involved in steps 3 and 4.[44-46] The increase in monocyte rolling and adhesion to the HUVEC endothelium in the presence of rFVIII under physiological flow conditions can be directly related to the observed overexpression of ICAM1, VCAM1 and E-selectin (Figure 2D). The transmigration assay

highlighted a donor-dependent effect of rFVIII that may be related to FVIII or VWF levels in donor blood, gender, or age.[68-71]

Neoangiogenesis and vascular remodeling have been reported in the development of hemophilic arthropathy.[72,73] This neoangiogenesis is characterized by the formation of large, irregular vessels, with an increase in the expression of vascular remodeling markers, such as αSMA, endoglin and VEGF.[74] These authors observed synovial neoangiogenesis in FVIII-deficient mice, with abnormal vascular architecture after induction of hemarthrosis. This vascular remodeling was maintained for several months, and also occurred on the control joint which did not have induced hemarthrosis. No similar phenomenon was observed in mice with osteoarthritis or rheumatoid arthritis, suggesting that it is specifically linked to FVIII deficiency.[74] Similar observations have been reported in patients.[72,73,75,76] The degree of arthropathy is greater in patients with hemophilia A than in those with hemophilia B (factor IX deficiency).[77] This observation underlines the functional impact of FVIII on the properties of the vascular barrier.

FVIII can regulate the biological properties of endothelial cells *in vitro*, with a functional impact on transcriptomic and protein profiles, vascular permeability, angiogenesis, monocyte adhesion, and transendothelial migration. However, the mechanisms of action of FVIII on endothelial cells remain to be defined to better manage bleeding and hemarthrosis in hemophilia patients. Although hemarthrosis can be reduced by replacement therapy, bleeding cannot be completely suppressed.[78,79] Despite prophylactic treatment with recombinant FVIII, 30 to 50% of hemophiliac patients suffer from hemophilic arthropathy.[80-82] The role played by thrombin generation in the functional impact observed in endothelial cells also remains to be explored. FXa also modulated vascular tube formation *in vitro* and *in vivo* in a mouse model of lower limb ischemia; inhibiting it with rivaroxaban restored angiogenesis.[83] In the context of hemophilia, the absence of FXa and thrombin caused by FVIII deficiency may then promote this abnormal angiogenesis.

References

1. Sturtzel C. Endothelial Cells (2017) Adv Exp Med Biol 1003:71-91. doi:10.1007/978-3-319-57613-8_4
2. Roumenina LT, Rayes J, Frimat M, Fremeaux-Bacchi V (2016) Endothelial cells: source, barrier, and target of defensive mediators. Immunol Rev 274(1):307-329. doi:10.1111/imr.12479
3. Rodrigues M, Kosaric N, Bonham CA, Gurtner GC (2019) Wound Healing: A Cellular Perspective. Physiol Rev 99(1):665-706. doi:10.1152/physrev.00067.2017

4. Cadé M, Muñoz-Garcia J, Babuty A, Fouassier M, Heymann MF, Monahan PE, Heymann D (2021) FVIII at the crossroad of coagulation, bone and immune biology: emerging evidence of biological activities beyond hemostasis. Drug Discov Today. Published online July 23, 2021:S1359-6446(21)00321-4. doi:10.1016/j.drudis.2021.07.015
5. Gerhardt T, Ley K (2015) Monocyte trafficking across the vessel wall. Cardiovasc Res 107(3):321-330. doi:10.1093/cvr/cvv147
6. Lenting PJ, Christophe OD, Guéguen P (2010) The disappearing act of factor VIII. Haemophilia 16(102):6-15. doi:10.1111/j.1365-2516.2008.01864.x
7. Kamikubo Y, Mendolicchio GL, Zampolli A, et al (2017) Selective factor VIII activation by the tissue factor-factor VIIa-factor Xa complex. Blood. 130(14):1661-1670. doi:10.1182/blood-2017-02-767079
8. Mertens K, Bertina RM (1982) Activation of human coagulation factor VIII by activated factor X, the common product of the intrinsic and the extrinsic pathway of blood coagulation. Thromb Haemost 47(2):96-100.
9. Nogami K, Shima M, Hosokawa K, et al (1999) Role of Factor VIII C2 Domain in Factor VIII Binding to Factor Xa. J Biol Chem 274(43):31000-31007. doi:10.1074/jbc.274.43.31000
10. Pryzdial ELG, Lee FMH, Lin BH, Carter RLR, Tegegn TZ, Belletrutti MJ (2018) Blood coagulation dissected. Transfus Apher Sci 57(4):449-457. doi:10.1016/j.transci.2018.07.003
11. Sang Y, Roest M, de Laat B, de Groot PG, Huskens D (2021) Interplay between platelets and coagulation. Blood Rev 46:100733. doi:10.1016/j.blre.2020.100733
12. Pipe SW, Montgomery RR, Pratt KP, Lenting PJ, Lillicrap D (2016) Life in the shadow of a dominant partner: the FVIII-VWF association and its clinical implications for hemophilia A. Blood 128(16):2007-2016. doi:10.1182/blood-2016-04-713289
13. Groth CG, Hathaway WE, Gustafsson A,Geis WP, Putnam CW, Björkén C, Porter KA, Starzl TE (1974) Correction of coagulation in the hemophilic dog by transplantation of lymphatic tissue. Surgery 75(5):725-733.
14. Veltkamp JJ, Asfaou E, van de Torren K, van der Does JA, van Tilburg NH, Pauwels EK (1974) Extrahepatic factor VIII synthesis. Lung transplants in hemophilic dogs. Transplantation 18(1):56-62. doi:10.1097/00007890-197407000-00009
15. Webster WP, Zukoski CF, Hutchin P, Reddick RL, Mandel SR, Penick GD (1971) Plasma factor VIII synthesis and control as revealed by canine organ transplantation. Am J Physiol 220(5):1147-1154. doi:10.1152/ajplegacy.1971.220.5.1147
16. Pan J, Dinh TT, Rajaraman A, et al (2016) Patterns of expression of factor VIII and von Willebrand factor by endothelial cell subsets in vivo. Blood 128(1):104-109. doi:10.1182/blood-2015-12-684688
17. Jacquemin M, Neyrinck A, Hermanns MI, et al (2006) FVIII production by human lung microvascular endothelial cells. Blood 108(2):515-517. doi:10.1182/blood-2005-11-4571
18. Fahs SA, Hille MT, Shi Q, Weiler H, Montgomery RR (2014) A conditional knockout mouse model reveals endothelial cells as the principal and possibly exclusive source of plasma factor VIII. Blood 123(24):3706-3713. doi:10.1182/blood-2014-02-555151
19. Mao H, Lockyer P, Townley-Tilson WHD, Xie L, Pi X (2016) LRP1 Regulates Retinal Angiogenesis by Inhibiting PARP-1 Activity and Endothelial Cell Proliferation. Arterioscler Thromb Vasc Biol 36(2):350-360. doi:10.1161/ATVBAHA.115.306713
20. Pi X, Schmitt CE, Xie L, et al (2012) LRP1-dependent endocytic mechanism governs the signaling output of the bmp system in endothelial cells and in angiogenesis. Circ Res 111(5):564-574. doi:10.1161/CIRCRESAHA.112.274597

21. Lenting PJ, Neels JG, van den Berg BM, et al (1999) The light chain of factor VIII comprises a binding site for low density lipoprotein receptor-related protein. J Biol Chem 274(34):23734-23739. doi:10.1074/jbc.274.34.23734
22. Saenko EL, Yakhyaev AV, Mikhailenko I, Strickland DK, Sarafanov AG (1999) Role of the low density lipoprotein-related protein receptor in mediation of factor VIII catabolism. J Biol Chem 274(53):37685-37692. doi:10.1074/jbc.274.53.37685
23. András IE, Eum SY, Huang W, Zhong Y, Hennig B, Toborek M (2010) HIV-1-induced amyloid beta accumulation in brain endothelial cells is attenuated by simvastatin. Mol Cell Neurosci 43(2):232-243. doi:10.1016/j.mcn.2009.11.004
24. Pflanzner T, Janko MC, André-Dohmen B, et al (2011) LRP1 mediates bidirectional transcytosis of amyloid-β across the blood-brain barrier. Neurobiol Aging 32(12):2323.e1-11. doi:10.1016/j.neurobiolaging.2010.05.025
25. Storck SE, Meister S, Nahrath J, et al (2016) Endothelial LRP1 transports amyloid-β(1-42) across the blood-brain barrier. J Clin Invest 126(1):123-136. doi:10.1172/JCI81108
26. Benslimane-Ahmim Z, Heymann D, Dizier B, et al (2011) Osteoprotegerin, a new actor in vasculogenesis, stimulates endothelial colony-forming cells properties. J Thromb Haemost 9(4):834-843. doi:10.1111/j.1538-7836.2011.04207.x
27. Muñoz-Garcia J, Mazza M, Alliot C, Sinquin C, Colliec-Jouault S, Heymann D, Huclier-Markai S (2021) Antiproliferative Properties of Scandium Exopolysaccharide Complexes on Several Cancer Cell Lines. Mar Drugs 19(3):174. doi:10.3390/md19030174
28. Dobin A, Davis CA, Schlesinger F, et al (2013) STAR: ultrafast universal RNA-seq aligner. Bioinformatics 29(1):15-21. doi: 10.1093/bioinformatics/bts635.
29. Liao Y, Smyth GK, Shi W (2019) The R package Rsubread is easier, faster, cheaper and better for alignment and quantification of RNA sequencing reads. Nucleic Acids Res 47:e47. doi: 10.1093/nar/gkz114
30. Love MI, Huber W, Anders S (2014) Moderated estimation of fold change and dispersion for RNA-seq data with DESeq2. Genome Biol 2014;15:550. doi: 10.1186/s13059-014-0550-8.
31. Shannon P, Markiel A, Ozier O, et al (2003) Cytoscape: a software environment for integrated models of biomolecular interaction networks. Genome Res 13(11):2498-504
32. Jensen LJ, Kuhn M, Stark M, et al (2009) STRING 8-a global view on proteins and their functional interactions in 630 organisms. Nucleic Acids Res 37(Database issue):D412-6. doi: 10.1093/nar/gkn760.
33. Bader GD, Hogue CW (2003) An automated method for finding molecular complexes in large protein interaction networks. BMC Bioinformatics 13;4:2. doi: 10.1186/1471-2105-4-2.
34. Zemani F, Silvestre J-S, Fauvel-Lafeve F, et al (2008) Ex vivo priming of endothelial progenitor cells with SDF-1 before transplantation could increase their proangiogenic potential. Arterioscler Thromb Vasc Biol 28(4):644-650. doi:10.1161/ATVBAHA.107.160044
35. Ségaliny AI, Mohamadi A, Dizier B, et al (2015) Interleukin-34 promotes tumor progression and metastatic process in osteosarcoma through induction of angiogenesis and macrophage recruitment. Int J Cancer 137(1):73-85. doi:10.1002/ijc.29376
36. Dias JV, Benslimane-Ahmim Z, Egot M, et al (2012) A motif within the N-terminal domain of TSP-1 specifically promotes the proangiogenic activity of endothelial colony-forming cells. Biochem Pharmacol 84(8):1014-1023. doi:10.1016/j.bcp.2012.07.006
37. Vandenhaute E, Drolez A, Sevin E, Gosselet F, Mysiorek C, Dehouck MP (2016) Adapting coculture in vitro models of the blood–brain barrier for use in cancer research:

maintaining an appropriate endothelial monolayer for the assessment of transendothelial migration. Laboratory Investigation 96(5):588-598. doi:10.1038/labinvest.2016.35
38. Heymann D, Kerdraon O, Verriele V, et al (2020) Centre de Ressources Biologiques-Tumorothèque: Bioresources and Associated Clinical Data Dedicated to Translational Research in Oncology at the Institut de Cancérologie de l'Ouest, France. Open J Biores 7(1):5. doi:10.5334/ojb.62
39. Madge LA, Pober JS (2001) TNF Signaling in Vascular Endothelial Cells. Exp Mol Pathol 70(3):317-325. doi:10.1006/exmp.2001.2368
40. Tellides G, Pober JS (2007) Interferon-γ Axis in Graft Arteriosclerosis. Circulation Res 100(5):622-632. doi:10.1161/01.RES.0000258861.72279.29
41. Pollard TD, Borisy GG (2003) Cellular motility driven by assembly and disassembly of actin filaments. Cell 112(4):453-465. doi:10.1016/s0092-8674(03)00120-x
42. Svitkina T (2018) The Actin Cytoskeleton and Actin-Based Motility. Cold Spring Harb Perspect Biol 10(1). doi:10.1101/cshperspect.a018267
43. Bellis SL, Miller JT, Turner CE (1995) Characterization of Tyrosine Phosphorylation of Paxillin in Vitro by Focal Adhesion Kinase. J Biol Chem 270(29):17437-17441. doi:10.1074/jbc.270.29.17437
44. Greenwood J, Wang Y, Calder VL (1995) Lymphocyte adhesion and transendothelial migration in the central nervous system: the role of LFA-1, ICAM-1, VLA-4 and VCAM-1. off. Immunol 86(3):408-415.
45. Lehmann JCU, Jablonski-Westrich D, Haubold U, Gutierrez-Ramos J-C, Springer T, Hamann A (2003) Overlapping and selective roles of endothelial intercellular adhesion molecule-1 (ICAM-1) and ICAM-2 in lymphocyte trafficking. J Immunol 171(5):2588-2593. doi:10.4049/jimmunol.171.5.2588
46. Jones RT, Toledo-Pereyra LH, Quesnelle KM (2015) Selectins in Liver Ischemia and Reperfusion Injury. J Invest Surg 28(5):292-300. doi:10.3109/08941939.2015.1056920
47. Kang L, Shen L, Lu L, et al (2019) Asparaginyl endopeptidase induces endothelial permeability and tumor metastasis via downregulating zonula occludens protein ZO-1. Biochim Biophys Acta Mol Basis Dis 1865(9):2267-2275. doi:10.1016/j.bbadis.2019.05.003
48. Tornavaca O, Chia M, Dufton N, et al (2015) ZO-1 controls endothelial adherens junctions, cell-cell tension, angiogenesis, and barrier formation. J Cell Biol 208(6):821-838. doi:10.1083/jcb.201404140
49. van der Flier A, Sonnenberg A (2001) Function and interactions of integrins. Cell Tissue Res 305(3):285-298. doi:10.1007/s004410100417
50. Legate KR, Fässler R (2009) Mechanisms that regulate adaptor binding to beta-integrin cytoplasmic tails. J Cell Sci 122(Pt 2):187-198. doi:10.1242/jcs.041624
51. Quadri SK (2012) Cross talk between focal adhesion kinase and cadherins: role in regulating endothelial barrier function. Microvasc Res 83(1):3-11. doi:10.1016/j.mvr.2011.08.001
52. German AE, Mammoto T, Jiang E, Ingber DE, Mammoto A (2014) Paxillin controls endothelial cell migration and tumor angiogenesis by altering neuropilin 2 expression. J Cell Sci 127:1672-1683. doi:10.1242/jcs.132316
53. Hu Y-L, Lu S, Szeto KW, et al (2014) FAK and paxillin dynamics at focal adhesions in the protrusions of migrating cells. Sci Rep 4(1):6024. doi:10.1038/srep06024
54. López-Colomé AM, Lee-Rivera I, Benavides-Hidalgo R, López E (2017) Paxillin: a crossroad in pathological cell migration. J Hematol Oncol 10. doi:10.1186/s13045-017-0418-y

55. Alday-Parejo B, Ghimire K, Coquoz O, et al (2021) MAGI1 localizes to mature focal adhesion and modulates endothelial cell adhesion, migration and angiogenesis. Cell Adh Migr 15(1):126-139. doi:10.1080/19336918.2021.1911472
56. Choi CK, Vicente-Manzanares M, Zareno J, Whitmore LA, Mogilner A, Horwitz AR (2008) Actin and α-actinin orchestrate the assembly and maturation of nascent adhesions in a myosin II motor-independent manner. Nature Cell Biol 10(9):1039-1050. doi:10.1038/ncb1763
57. Parsons JT, Horwitz AR, Schwartz MA (2010) Cell adhesion: integrating cytoskeletal dynamics and cellular tension. Nature Rev Mol Cell Biol 11(9):633-643. doi:10.1038/nrm2957
58. Friedl P, Wolf K (2003) Tumour-cell invasion and migration: diversity and escape mechanisms. Nat Rev Cancer 3(5):362-374. doi:10.1038/nrc1075
59. Gupton SL, Waterman-Storer CM (2006) Spatiotemporal feedback between actomyosin and focal-adhesion systems optimizes rapid cell migration. Cell 125(7):1361-1374. doi:10.1016/j.cell.2006.05.029
60. Mogilner A, Keren K (2009) The shape of motile cells. Curr Biol 19(17):R762-771. doi:10.1016/j.cub.2009.06.053
61. Parri M, Chiarugi P (2010) Rac and Rho GTPases in cancer cell motility control. Cell Commun Signal 8:23. doi:10.1186/1478-811X-8-23
62. Natale CF, Lafaurie-Janvore J, Ventre M, Babataheri A, Barakat AI. Focal adhesion clustering drives endothelial cell morphology on patterned surfaces (2019) J R Soc Interface 16(158). doi:10.1098/rsif.2019.0263
63. Sjöblom B, Salmazo A, Djinović-Carugo K (2008) Alpha-actinin structure and regulation. Cell Mol Life Sci 65(17):2688-2701. doi:10.1007/s00018-008-8080-8
64. Fanning AS, Jameson BJ, Jesaitis LA, Anderson JM (1998) The tight junction protein ZO-1 establishes a link between the transmembrane protein occludin and the actin cytoskeleton. J Biol Chem 273(45):29745-29753. doi:10.1074/jbc.273.45.29745
65. Yamamoto T, Saeki Y, Kurasawa M, Kuroda S, Arase S, Sasaki H (2008) Effect of RNA interference of tight junction-related molecules on intercellular barrier function in cultured human keratinocytes. Arch Dermatol Res 300(9):517-524. doi:10.1007/s00403-008-0868-8
66. Aird WC (2007) Phenotypic heterogeneity of the endothelium: I. Structure, function, and mechanisms. Circ Res 100(2):158-173. doi:10.1161/01.RES.0000255691.76142.4a
67. Cerutti C, Ridley AJ (2017) Endothelial cell-cell adhesion and signaling. Experimental Cell Res 358(1):31-38. doi:10.1016/j.yexcr.2017.06.003
68. Loon JE van, Kavousi M, Leebeek FWG, et al (2012) von Willebrand factor plasma levels, genetic variations and coronary heart disease in an older population. J Thromb Haemostasis 10(7):1262-1269. doi:10.1111/j.1538-7836.2012.04771.x
69. Desch KC (2018) Regulation of plasma von Willebrand factor. F1000Res 7:96. doi:10.12688/f1000research.13056.1
70. Viel KR, Machiah DK, Warren DM, et al (2007) A sequence variation scan of the coagulation factor VIII (FVIII) structural gene and associations with plasma FVIII activity levels. Blood 109(9):3713-3724. doi:10.1182/blood-2006-06-026104
71. Turecek PL, Johnsen JM, Pipe SW, O'Donnell JS, iPATH study group (2020) Biological mechanisms underlying inter-individual variation in factor VIII clearance in haemophilia. Haemophilia 26(4):575-583. doi:10.1111/hae.14078
72. Acharya SS, Kaplan RN, Macdonald D, Fabiyi OT, DiMichele D, Lyden D (2011) Neoangiogenesis contributes to the development of hemophilic synovitis. Blood 117(8):2484-2493. doi:10.1182/blood-2010-05-284653

73. Zetterberg E, Palmblad J, Wallensten R, Morfini M, Melchiorre D, Holmström M (2014) Angiogenesis is increased in advanced haemophilic joint disease and characterised by normal pericyte coverage. Eur J Haematol 92(3):256-262. doi:10.1111/ejh.12227
74. Bhat V, Olmer M, Joshi S, et al (2015) Vascular remodeling underlies rebleeding in hemophilic arthropathy. Am J Hematol 90(11):1027-1035. doi:10.1002/ajh.24133
75. Kidder W, Chang EY, Moran CM, Rose SC, von Drygalski A (2016) Persistent Vascular Remodeling and Leakiness are Important Components of the Pathobiology of Re-bleeding in Hemophilic Joints: Two Informative Cases. Microcirculation 23(5):373-378. doi:https://doi.org/10.1111/micc.12273
76. Mauser-Bunschoten EP, Zijl JAC, Mali W, van Rinsum AC, van den Berg HM, Roosendaal G (2005) Successful treatment of severe bleeding in hemophilic target joints by selective angiographic embolization. Blood 105(7):2654-2657. doi:10.1182/blood-2004-06-2063
77. Melchiorre D, Linari S, Manetti M, et a (2016) Clinical, instrumental, serological and histological findings suggest that hemophilia B may be less severe than hemophilia A. Haematologica 101(2):219-225. doi:10.3324/haematol.2015.133462
78. Mingot-Castellano ME (2019) Clinical pattern of hemophilia and causes of variability. Blood Coagul Fibrinolysis 30:S4-S6. doi:10.1097/MBC.0000000000000821
79. Zimmerman B, Valentino LA (2013) Hemophilia: in review. Pediatr Rev 34(7):289-294; quiz 295. doi:10.1542/pir.34-7-289
80. Aznar JA, Lucía F, Abad-Franch L, et al (2009) Haemophilia in Spain. Haemophilia. 15(3):665-675. doi:10.1111/j.1365-2516.2009.02001.x
81. Jackson SP (2007) The growing complexity of platelet aggregation. Blood. 109(12):5087-5095. doi:10.1182/blood-2006-12-027698
82. Schramm W, Gringeri A, Ljung R, et al (2012) Haemophilia care in Europe: the ESCHQoL study. Haemophilia 18(5):729-737. doi:10.1111/j.1365-2516.2012.02847.x
83. Sanada F, Taniyama Y, Muratsu J, et al (2016) Activated Factor X Induces Endothelial Cell Senescence Through IGFBP-5. Sci Rep 6(1):35580. doi:10.1038/srep35580

Figure legends

Figure 1: rFVIII inhibits HUVEC adhesion. HUVECs (15,000 cells/well) were seeded in 96-multi-well electronic microplates (E-Plate 96) in EGM2 (**A)** or EBM2 (**B)** medium in the presence or absence of increasing concentrations of rFVIII. Cell index related to the cellular impedance was measured in real-time using the xCELLigence RTCA MP instrument. Mean cell index ± SEM of 3 or 4 independent experiments. * $p < 0.05$, ** $p < 0.01$.

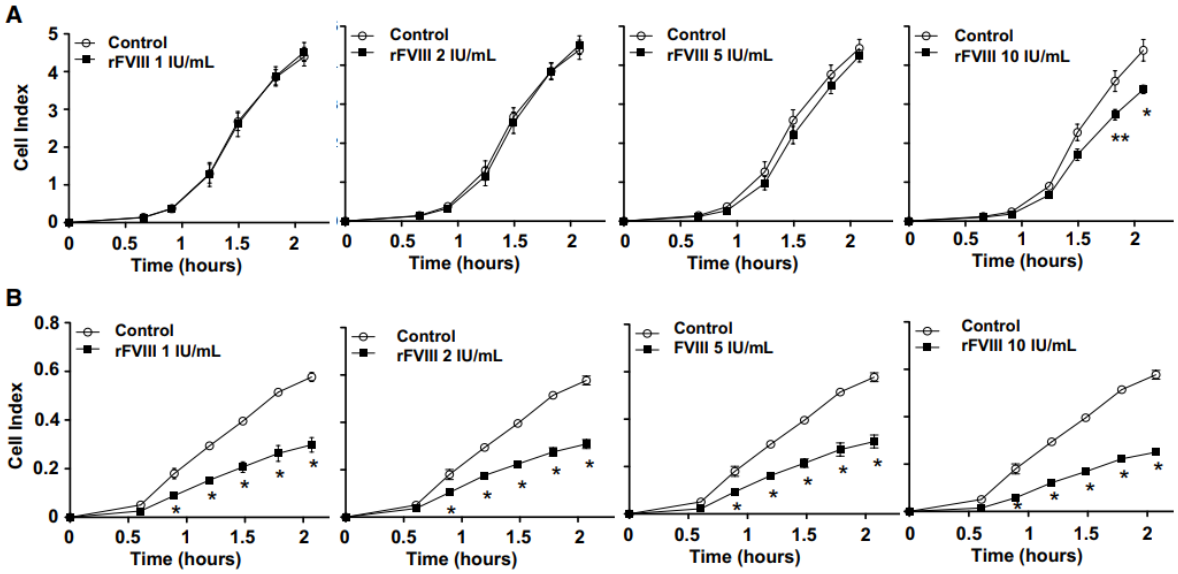

Figure 2: rFVIII, but not rOPG and rVWF modulates the transcriptomic profile of HUVECs. (A) PCA plot of three independent experiments. HUVECs were cultured in the presence or absence (CT, red points) of 10 UI/mL of rFVIII (green points), 100 ng/mL of rOPG (blue points), 50 ng/mL of rVWF (purple points) for 7 h; (**B)** Heatmap visualization of the z-scored expression of the 563 genes (|log2FC| > 1, p value adjusted <0.05) that were differentially expressed in rFVIII-treated cells compared to the other groups; (**C)** Volcano plot analysis of differentially expressed genes in rFVIII-treated HUVECs compared to the control group. The genes with 2-fold overexpression or underexpression appear in green and red respectively. (**D)** List of the 2-fold overexpressed and underexpressed genes. (**E)** Protein network generated with Cytoscape, showing the 563 proteins corresponding to the 563 differentially-expressed genes. Each point represents one protein, and each line represents one protein interaction. Red circles represent the overexpressed genes, and blue circles the underexpressed genes. The table summarizes the 10 main functional pathways related to the genes most significantly modulated by rFVIII.

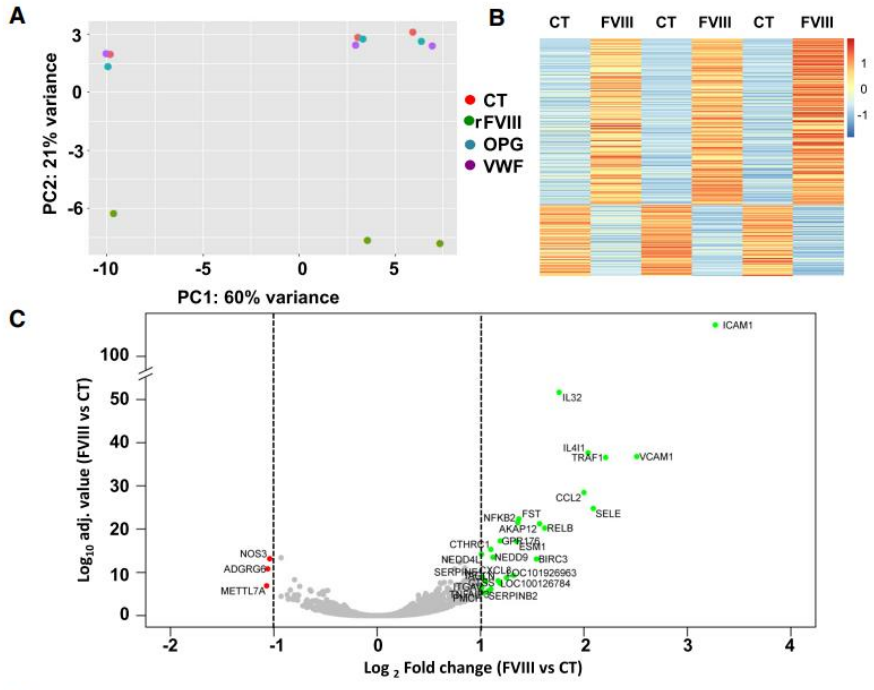

D

Gene	Fold change
ICAM1	9.6
VCAM1	5.6
TRAF1	4.6
SELE	4.2
IL4I1	4.1
CCL2	4
IL32	3.4
RELB	3.1
AKAP12	3
BIRC3	2.9
FST	2.6
NFKB2	2.6
ESM1	2.5
CXCL8	2.5
LOC101926963	2.4
GPR176	2.3
LOC100126784	2.3
TAGLN	2.2
NEDD9	2.2
CTHRC1	2.1
TNFAIP3	2.1
SERPINB2	2.1
ITGAV	2.1
PMCH	2
SERPINE1	2
NEDD4L	2
CTSS	2
SPOCD1	2
NOS3	-2
ADGRG6	-2.1
METTL7A	-2.1

E

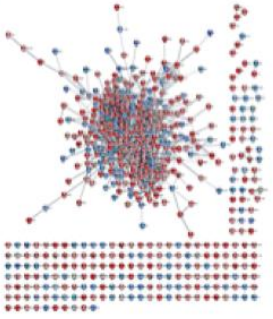

Number of genes regulated	Database	Enriched functions	p value
68	GO Process	Tube morphogenesis	4.45E-17
286	GO Function	Protein binding	2.78E-16
74	GO Process	Tube development	2.76E-15
405	GO Component	Cytoplasm	5.95E-14
314	GO Process	Response to stimulus	1.46E-13
68	GO Process	Regulation of cell migration	1.92E-13
71	GO Process	Anatomical structure formation involved in morphogenesis	4.42E-13
48	GO Component	Actin cytoskeleton	1.55E-12
150	GO Process	Response to organic substance	2.35E-12
133	GO Process	Immune system process	2.87E-12

Figure 3: rFVIII modifies the organization of the actin cytoskeleton and paxillin phosphorylation in endothelial cells and increases the permeability of the HUVEC endothelium. HUVECs were cultured over adhesive crossbow CytooChip™ micropatterns and left to spread in the presence or absence of increasing doses of rFVIII for 18 h. The organization of the actin fibers and the localization of phospho-PAX were analyzed in HUVECs polarized on each micropattern using immunocytochemistry. **A)** Actin stress fibers and the actin network were observed at the retraction and protrusion zones respectively. Standardized images of actin fibers (in green) observed at the retraction of single cells treated with different concentrations of rFVIII. White arrow: directional polarity and migration. (**B**) From each cell analyzed, quantification of the F-actin-stained surface was determined using confocal microscopy coupled to Image J analysis: total stained surface and surface of one fiber (fiber-stained surface) in μm^2. $n \geq 23$ per condition. (**C)** Standardized images of P-PAX (in red) observed at the retraction zone where mature focal adhesions were formed. (**D)** Standardized images of P-PAX at the protrusion zone. Cell ruffling takes place at the front of cell migration. **(E**) Histograms representing the P-PAX surface stained per cell (Total stained surface), the mean surface per phosphorylated event (Mean stained surface), the number of phosphorylated events (Number of events) and the perimeter of each phosphorylated event (Perimeter of events). Mean ± SEM, $n \geq 65$ per condition. Mean ± SEM, one way ANOVA * < 0.05, ** < 0.01, *** < 0.001.

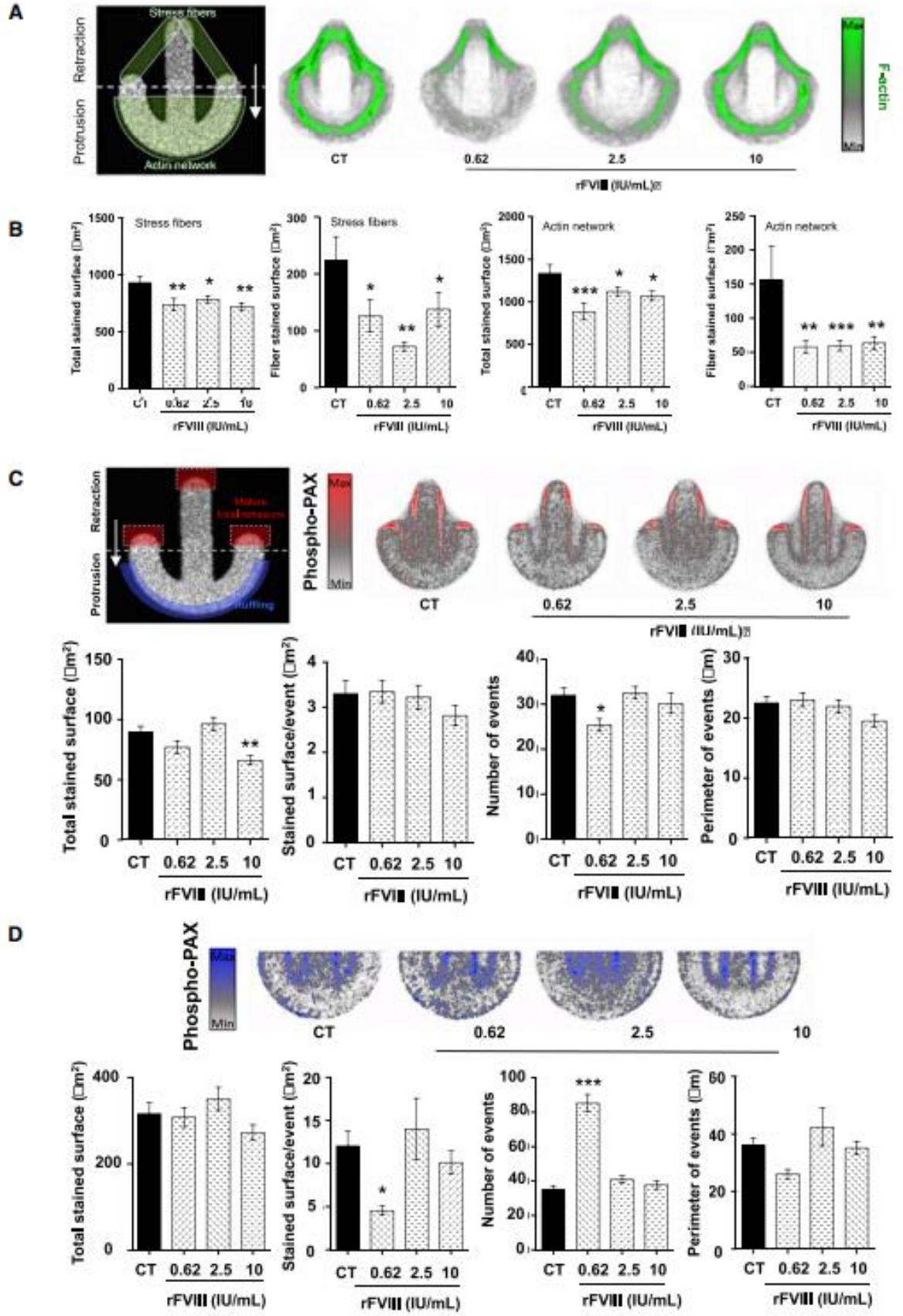
A
Stress fibers
Retraction
Protrusion
Actin network
CT
0.62
2.5
10
rFVIII (IU/mL)
Max
Min
F-actin
B
Stress fibers
Total stained surface (□m²)
Fiber stained surface (□m²)
Actin network
CT
0.62
2.5
10
rFVIII (IU/mL)
C
Retraction
Protrusion
Phospho-PAX
Max
Min
CT
0.62
2.5
10
rFVIII (IU/mL)
Total stained surface (□m²)
Stained surface/event (□m²)
Number of events
Perimeter of events (□m)
D
Phospho-PAX
Max
Min
CT
0.62
2.5
10
Total stained surface (□m²)
Stained surface/event (□m²)
Number of events
Perimeter of events (□m)
rFVIII (IU/mL)

Figure 4: rFVIII increases the vascular permeability: functional relationship with decreased ZO-1 expression at the surface of the HUVEC endothelium. (**A**) HUVECs were seeded on fibronectin-coated inserts. After 3 days of culture, vehicle (black curves) or 2.5, 5, 10 or 20 IU/mL of rFVIII (red line) or 10 ng/mL of TNF-α (green line) were added to the upper compartment of the insert concomitantly to a solution of 250 µg/mL of FITC-labeled dextran (70 kDa). The flux of FITC-labeled dextran through the HUVEC monolayer was determined in the medium collected from the bottom compartment using a Victor 3 reader (excitation 485 nm, emission 520 nm). Mean FITC-labeled dextran concentration ± SEM of an experiment carried out in 6 replicates, Kruskall-Wallis test, * $p < 0.05$ compared to the control condition. (**B**) HUVECs were cultured over adhesive arena CytooChip™ micropatterns and left to spread in the presence or absence or increasing doses of rFVIII for 18 h. ZO-1 expression was assessed using immunocytochemistry. (**A**) ZO-1 immunostaining (in red), nuclei observed after DAPI staining (in blue). Overview of thresholding for the quantification of the ZO-1 surface, in greyscale (right panel). (**B**) Quantification of total ZO-1 staining surface per disc in µm² (left), staining surface per event in µm² (middle) and number of events (right). Mean ± SEM, n = 24 discs per condition, Kruskall-Wallis test. * < 0.05, ** < 0.01, *** < 0.001.

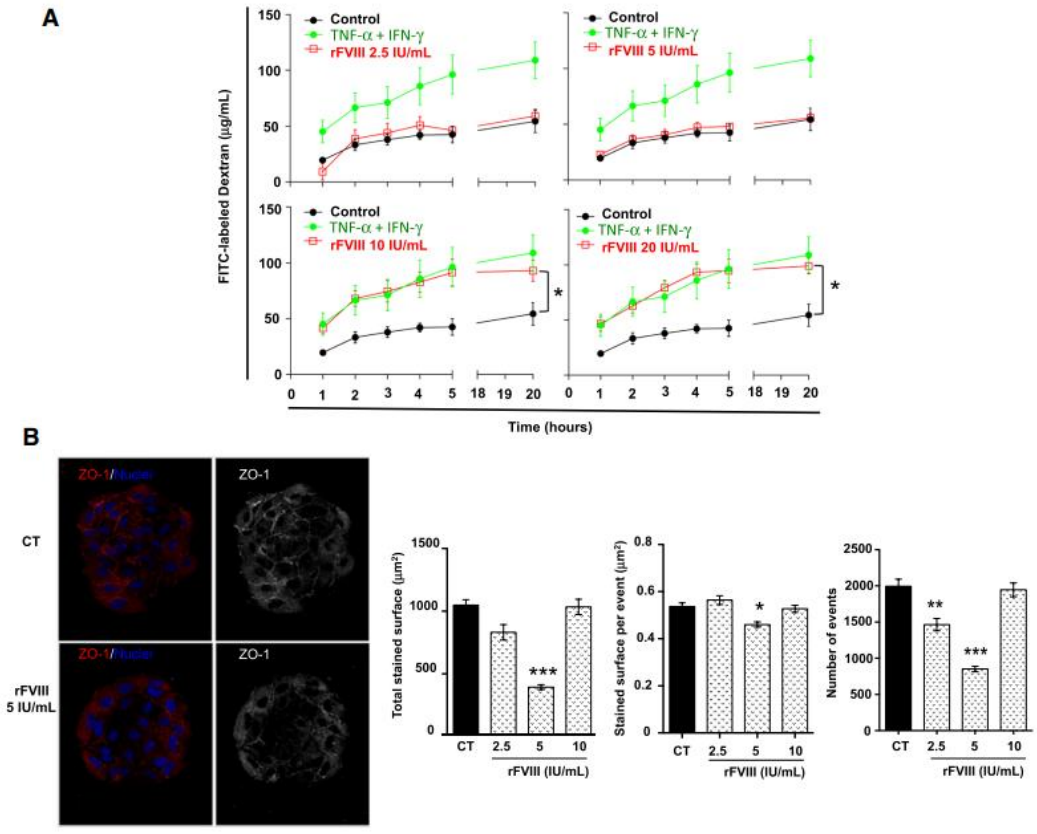

Figure 5: Human monocyte rolling on the HUVEC endothelium and monocyte transendothelial migration are enhanced by rFVIII. Calcein-labeled freshly isolated human monocytes or HUVEC endothelium were treated or not with 10 IU/mL of rFVIII for 6 h and 24 h respectively. Monocytes were perfused over the endothelium at 0.1 mL/min. One image per second was captured for 1.5 minutes on a central field. (**A)** Images of rolling monocytes (in green) after 45 sec of perfusion. The white arrows show the rolling monocytes. The number of adherent monocytes per second was counted in the same field. The total number of tethered monocytes in the same field for 1.5 minutes was counted. Mean ± SEM of ≥ 257 images per condition. One-way ANOVA, *** < 0.001. **(B**) Freshly isolated human monocytes were labelled with calcein and then perfused over a confluent HUVEC monolayer previously activated at a shear rate of $50s^{-1}$. Monocytes and HUVEC endothelium were treated or not with 10 IU/mL of rFVIII for 6h and 24h respectively. Images were captured over the entire chamber (28 fields). Images of monocytes (in green) adherent to the HUVEC endothelium. The number of adherent monocytes was counted on each field (84 fields per condition). Mean ± SEM, one-way ANOVA, *** < 0.001. (**C**) HUVECs were cultured in collagen-coated chambers (8 µm pore size) for three days. Monocytes were isolated using negative selection from whole blood collected from donors. Monocytes were added to the upper compartment in the presence or absence of 10 IU/mL of rFVIII for 4.5 hours or 20 hours. A cocktail of cytokines composed of 15 ng/mL of MCP1 and 5 ng/mL of RANTES used as monocyte chemoattractants was added to the subcompartment. After transendothelial migration, monocytes were collected in the bottom chamber and counting using flow cytometry. The number of transmigrated monocytes is expressed as a percentage of monocytes collected after transendothelial migration compared to the untreated control.

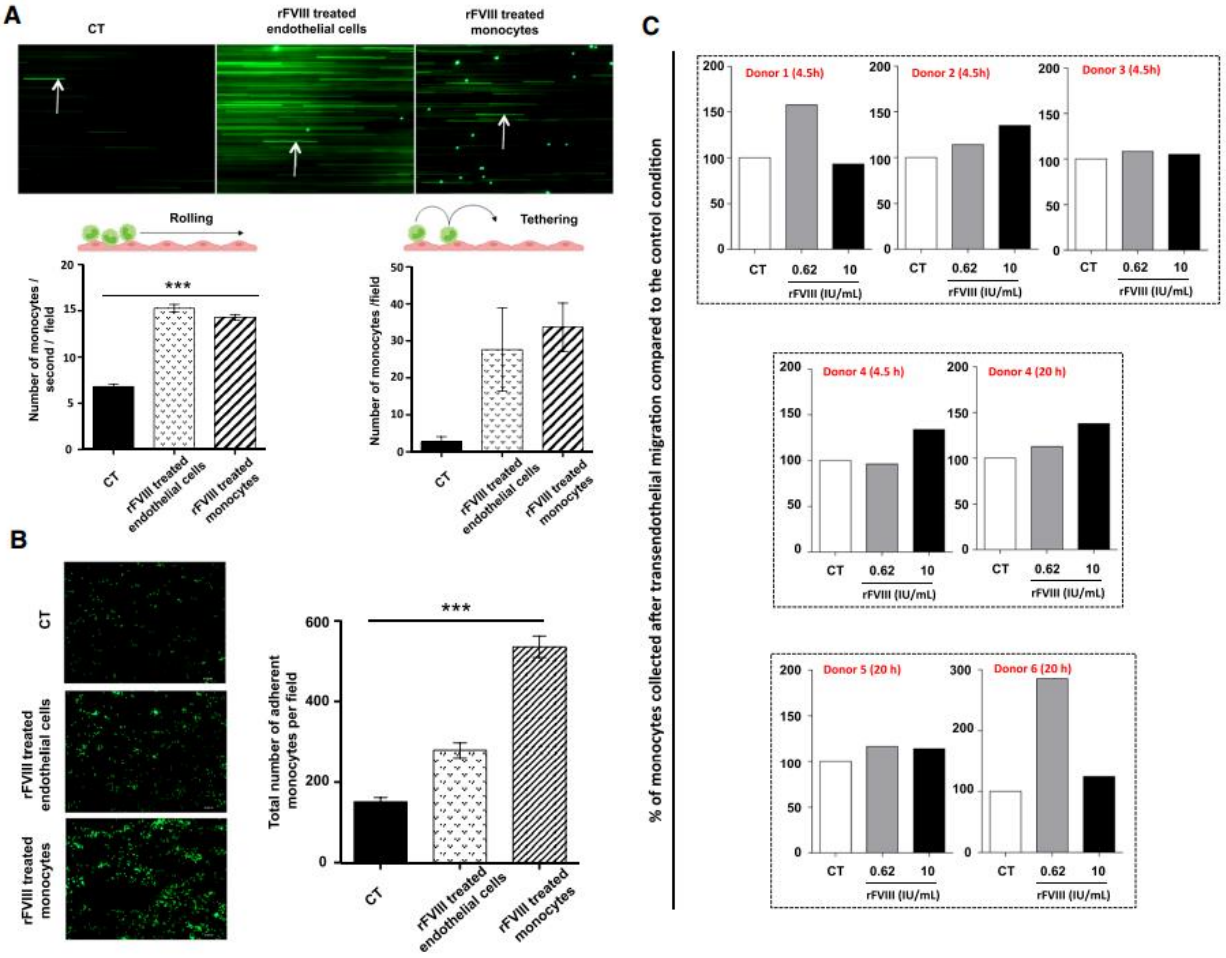
A
CT
rFVIII treated endothelial cells
rFVIII treated monocytes
Rolling
Tethering
Number of monocytes / second / field
***
Number of monocytes /field
CT
rFVIII treated endothelial cells
rFVIII treated monocytes
B
CT
rFVIII treated endothelial cells
rFVIII treated monocytes
Total number of adherent monocytes per field
***
C
% of monocytes collected after transendothelial migration compared to the control condition
Donor 1 (4.5h)
Donor 2 (4.5h)
Donor 3 (4.5h)
Donor 4 (4.5 h)
Donor 4 (20 h)
Donor 5 (20 h)
Donor 6 (20 h)
CT
0.62
10
rFVIII (IU/mL)

Table 1:

Immune profiling		Advanced profiling
Basal Condition	**inflammatory condition**	**Basal Condition**
rFVIII 2.5 IU/mL		
E-Sel **+18.2%**	HLA-1 **-48.30%**	c-MET **+18.5%**
TLR-4 **+27.29%**	HLA-2 **-25.40%**	
TNFR1 **+18.8%**		
rFVIII 5 IU/mL		
V-CAM-1 **+20.30%**	H-VEM **+17.4%**	CD41 **+17%**
E-Sel **+26.90%**	CD37L **+33.4%**	CD29 **+24%**
HLA-E **+15.5%**	HLA-1 **-24.8%**	Claudin-1 **-20.8%**
GTRL **-16.30%**		ZO-1 **-15.7%**
rFVIII 10 IU/mL		
ICAM-1 **+16%**	HLA-1 **+24.2%**	CD29 **+16.9%**
V-CAM **+20.3%**	HVEM **+16.5%**	
E-Sel **+22.9%**	CD37L **+22.6%**	
rFVIII 20 IU/mL		
ICAM-1 **+32%**	ICAM-1 **+16%**	EPCR **+36.1%**
MICA/B **+19.2%**	HVEM + **16.4%**	CD29 **+38.30%**
U		c-MET **+15.2%**
		LDL-Deg **+26.93%**
E		LDL-up **+37.88%**

HUVECs HUVEHUVECs were treated with increasing doses of rFVIII in the absence ("Basal condition") or presence ("inflammatory condition") of 10 ng/mL TNF-α or 20 ng/mL IFN-γ for 48h. Results are expressed as the percentage of modulation of each protein analyzed by flow cytometry

Supplementary figure 1: Functional predictive analysis of gene clusters modulated by rFVIII.

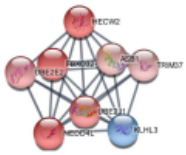

Genes regulated	Database	Enriched functions	p value
8	Reactome Pathways	Antigen processing: Ubiquitination & Proteasome degradation	9.66E-14
8	UniProt Keywords	Ubl conjugation pathway	8.55E-11
8	GO Process	protein ubiquitination	6.93E-10
6	GO Function	ubiquitin-protein transferase activity	7.33E-8
4	KEGG Pathways	Ubiquitin mediated proteolysis	1.13E-6

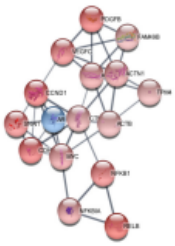

Genes regulated	Database	Enriched functions	p value
7	KEGG Pathways	Focal adhesion	1.49E-8
6	KEGG Pathways	Prostate cancer	1.49E-8
7	KEGG Pathways	HTLV-I infection	2.49E-8
5	KEGG Pathways	Adherens junction	7.66E-8
8	KEGG Pathways	Pathways in cancer	7.66E-8

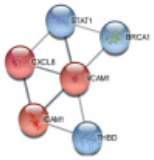

Genes regulated	Database	Enriched functions	p value
5	KEGG Pathways	AGE-RAGE signaling pathway in diabetic complications	1.31E-9
5	GO Process	cellular response to tumor necrosis factor	6.1E-7
4	Reactome Pathways	Interleukin-4 and Interleukin-13 signaling	1.33E-6
3	KEGG Pathways	Malaria	9.36E-6
4	GO Process	response to ionizing radiation	1.63E-5

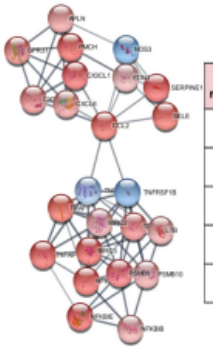

Genes regulated	Database	Enriched functions	p value
12	KEGG Pathways	TNF signaling pathway	3.15E-19
12	GO Process	Response to lipopolysaccharide	6.62E-13
9	Reactome Pathways	TNFR2 non-canonical NF-kB pathway	7.83E-13
14	GO Process	regulation of response to external stimulus	7.99E-12
8	KEGG Pathways	NF-kappa B signaling pathway	1.01E-11

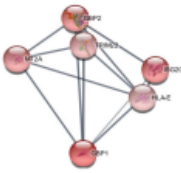

Genes regulated	Database	Enriched functions	p value
6	Reactome Pathways	Interferon Signaling	1.63E-11
5	Reactome Pathways	Interferon gamma signaling	1.05E-10
5	GO Process	interferon-gamma-mediated signaling pathway	1.71E-9
6	GO Process	cytokine-mediated signaling pathway	1.54E-7
6	GO Process	innate immune response	1.54E-7

Supplementary Figure 1: Functional predictive analysis of gene clusters modulated by rFVIII. RNA sequencing was carried out from HUVECs treated or not with 10 IU/mL of rFVIII for 7h. Five gene clusters were identified and String protein-protein interaction diagram of rFVIII regulated-gene clusters identified. Blue and red colored circles represent genes/ proteins dowregulated and upmodulated by rFVIII respectively. GO, KECK and Reactome term enrichment analysis of cellular components, biological processes and molecular functions was performed on each gene cluster. The tables summarize the five first enriched functional patways related to the corresponding clusters.

Supplementary Figure 2: FVIII regulates the expression of numerous proteins involved in vascular integrity, cell adhesion and immune fonctions.

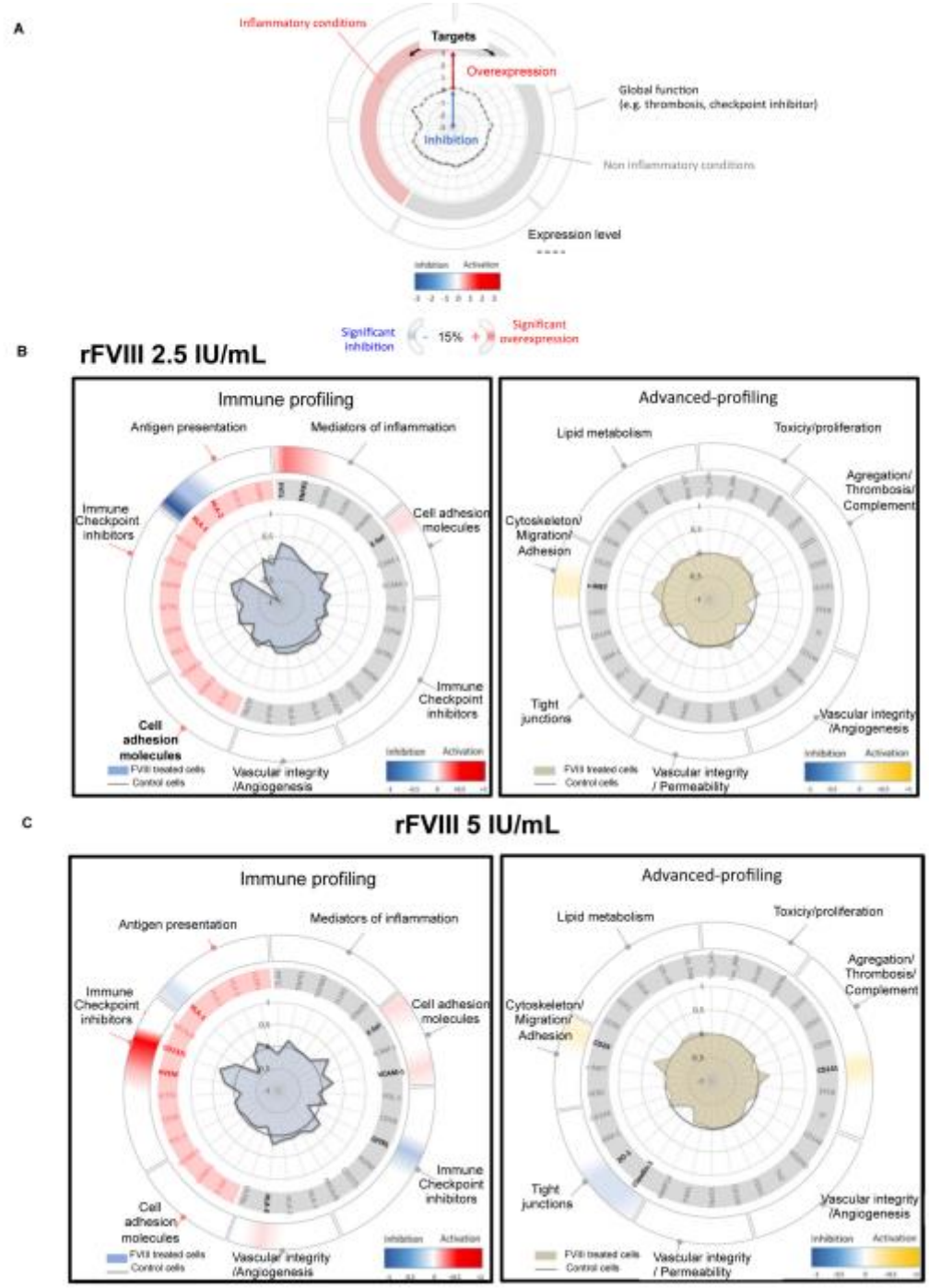

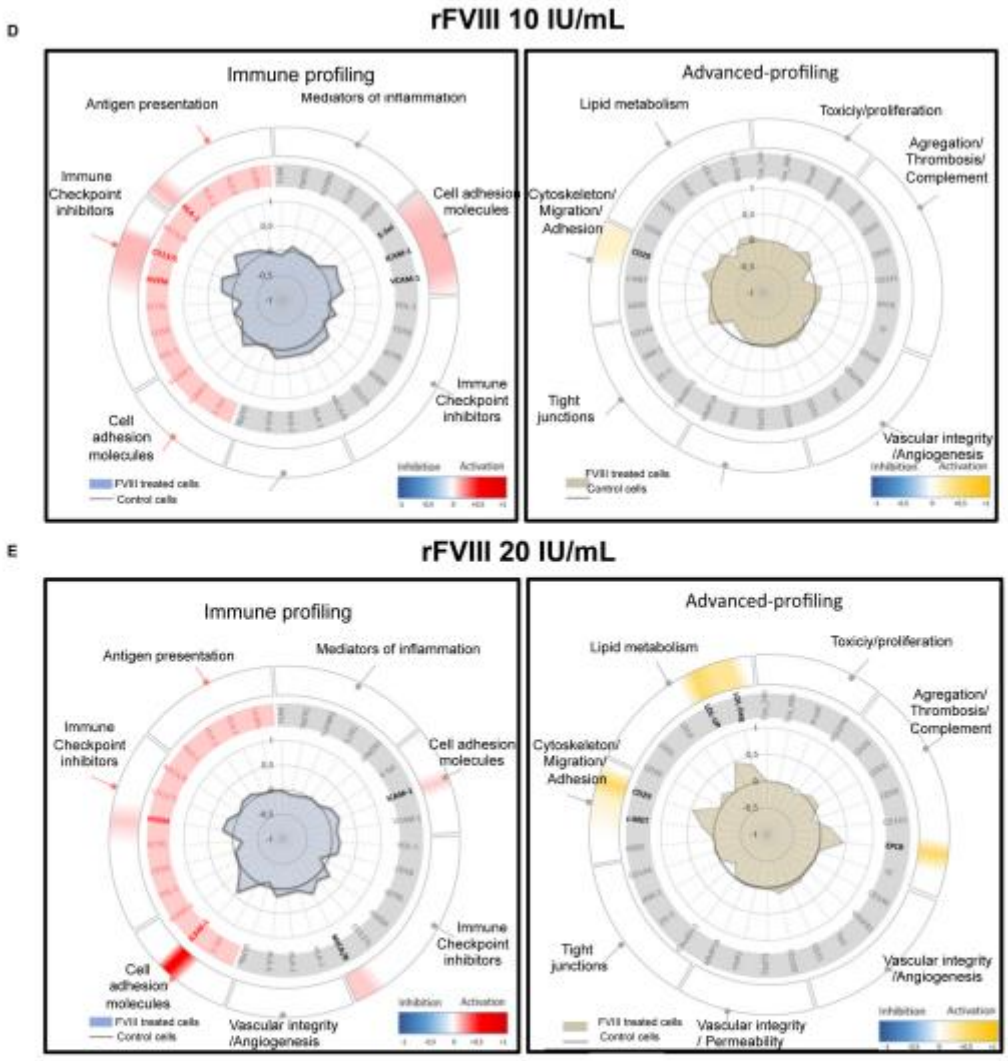

Supplementary Figure 2: FVIII regulates the expression of numerous proteins involved in vascular integrity, cell adhesion and immune functions. (**A**) Schematic diagrma expaling the reading of the panels. HUVECs were tretaed of not with 2.5 (**B**), 5 (**C**), 10 (**D**) or 20 (**E**) IU/mL) of rFVIII for 48 h. A modulation of +/- 15% in the presence of rFVIII comared to the control was considered significant. The proteins significantly modulated are indicated in bold in each panel.

Supplementary Figure 3: rFVIII mediates the vascular tubule formation *in vitro*

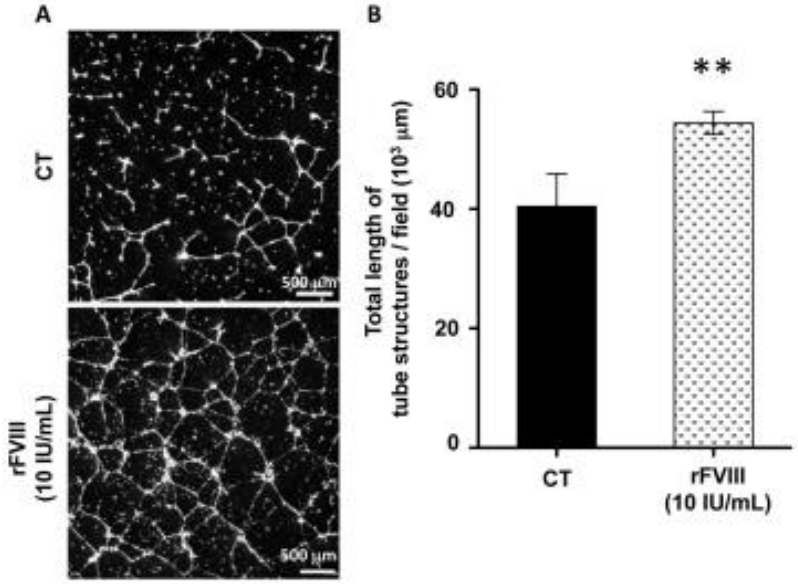

Supplementary Figure 3: rFVIII mediates the vascular tubule formation *in vitro*. After 24h of culture in basal medium, Endothelial colony-forming cells (ECFCs) were pretreated or not with 10 IU/mL of rFVIII and seeded on Matrigel® in growth factor-depleted basal medium. After 18h of culture the cells were fixed and stained with Giemsa. **(A)** Light-micrographs showing the typical appearance of tubules formed by control and rFVIII-pretreated ECFCs in Matrigel® (original magnification: x4). **(B)** Comparison of the mean (± SEM) total length of tubules (% of control ECFCs) analyzed by Fiji software with the "Angiogenesis Analyzer" plugin. ** $p < 0.01$ compared to the untreated cells.

Supplementary Figure 4: rFVIII does not modulate the resistance to detachment of human monocytes to HUVEC endothelium.

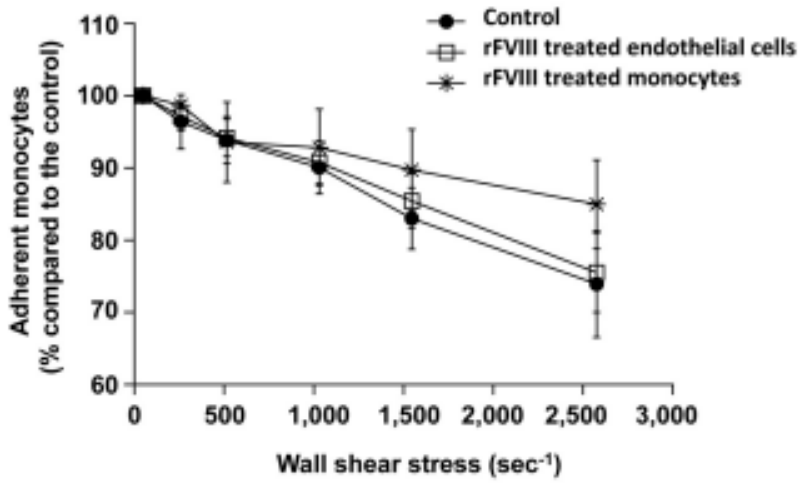

Supplementary Figure 4: rFVIII does not modulate the resistance to detachment of human monocytes to HUVEC endothelium. Adherent monocytes were tested for resistance x 5,000 to detachment from the preformed endothelium by increasing the flow rate from 50 to 5000 s^{-1} over 1 minute, and by counting the number of remaining adherent cells at one-minute intervals. Differential adherence between monocytes pretreated with 10 IU/mL of rFVIII-treated, or rFVIII-pretreated HUVECs and control cells at shear rates up to 2500 s^{-1}. Values are mean ± SEM.

Supplementary figure 5 : rFVIII speeds up the monocyte adherence to endothelial cells

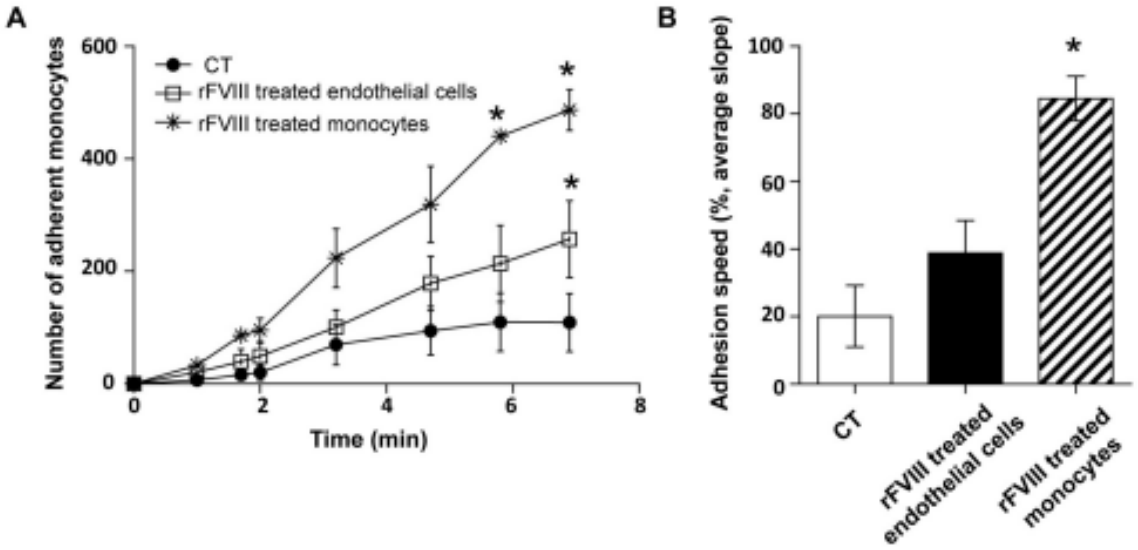

Supplementary Figure 5: rFVIII speeds up the monocyte adherence to endothelial cells. Calcein-labeled freshly isolated monocytes were perfused (0.1 mL/min) on HUVEC endothelium monolayers pretreated or not with 10 IU/mL of rFVIII. (**A**) A kinetic of monocyte adhesion was determined from regular captured images for 7 min. (**B**) Slope of each kinetic curve presented in (A). Mean ± SEM of three independent experiments. Kurskall-Wallis test. $p < 0.05$ compared to the untreated control cells.

Declarations

*** Ethics approval and consent to participate**: The study was performed in accordance with the ethical standards as laid down in the 1964 Declaration of Helsinki and its later amendments or comparable ethical standards. Blood sampling was coordinated by the Biological Ressource Center of the Institut de cancérologie de l'Ouest (CRB-Tumorothèque ICO). All samples processed by the CRB-Tumorothèque ICO were subject to the donor's agreement and the signing of informed consent. All samples collected were anonimized before release. The CRB-Tumorothèque ICO is committed to destroying samples and related information at the request of the donor. The activities of the CRB-Tumorothèque ICO are in accordance with the French legislation (especially the law of bioethics, 7th July 2011, and the chapter IV of the Public Health Code that gather all regulations for biobanks). They meet the ethical and regulatory requirements that govern the collection, conservation and use of biological samples for scientific purposes; this includes, according to article L.1243-3 of the Public Health Code, approval of the collection from a competent research ethics committee (CPP, "Comité de protection des personnes" in French) and obligation to respect donor's

informed consent in any access request to the samples. In addition, the CRB-Tumorothèque ICO works in respect to the national ethical chart reedited in 2010. All bioresources deposited at CRB-Tumorothèque ICO have been declared to and authorized by the French Research Ministry (Declaration Number: DC-2018-3321). This declaration includes approval by a research ethics committee.

* **Consent for publication:** With the submission of this manuscript we would like to undertake that all authors of this paper have read and approved the final version submitted. We confirm that the contents of this manuscript are not under consideration for publication elsewhere.

*** Availability of data and material**: The main data generated and analysed during this study are included in this published article and its supplementary information files. However, complementary datasets generated during and/or analysed during the current study are also available from the corresponding author on reasonable request.

*** Competing interests**: CNRS paid the salary of Dr C. Boisson-Vidal**.** Karim Fekir and Mathias Chatelais are employees of ProfileHIT (Sainte-Pazanne, France)

*** Funding:** The present work was supported by Shire (Recipient: Prof. D. Heymann, Institut de Cancérologie de l'Ouest, Saint-Herblain, France

*** Authors' contributions**. Authors contributed to the work as follow: MC, JMG, AB, DC, MFH contributed to the main part of the work including cell adhesion, migration, flow cytometry, functional assays, proteins, RNA and cell preparation; LP gave his expertise in bioinformatics and transcriptomic analysis; FK and MC contributed to the protein profiling and functional assays of endothelial cells; AL and CDV the contributed to the shear-flow adhesion assay. DH coordinated the works, wrote the manuscript that have been corrected and approved by all authors.

* **Acknowledgements:** We would like to thank Dr Aurélien Sérandour (Inserm, CRCINA) for his advice concerning the transcriptomic analyses. We acknowledge the MicroPICell facility, SFR-Santé, INSERM, CNRS, UNIV Nantes, CHU Nantes, Nantes, France, member of the

national infrastructure France-BioImaging supported by the French National Research Agency (ANR-10-INBS-04).